*Chinese Journal of*
**POLYMER SCIENCE**

ARTICLE

https://doi.org/10.1007/s10118-018-2048-4
*Chinese J. Polym. Sci.* 2018, 36, 521–527

# Synthesis, UV-curing Behavior and Surface Properties of New Fluorine-containing Aromatic Oxetane Monomers

Shu-Qing Fang, Yu-Lian Pang, and Ying-Quan Zou*

*College of Chemistry, Beijing Normal University, Beijing 100875, China*

**Abstract** In this paper, we combined high-end cationic UV-curable material with fluorinated chain obtaining a series of new fluorine-containing aromatic oxetane monomers *via* a mild nucleophilic substitution reaction. The structures and properties of monomers were characterized using $^{1}$H-NMR, $^{19}$F-NMR, dynamic viscosity tests and differential scanning calorimetry (DSC). It was determined that all of the fluorinated monomers obtained had much lower viscosity and higher thermostability after the introduction of hexafluorobenzene. Then, UV-curable coatings were prepared using four fluorine-containing aromatic oxetane monomers (FOX1–4); the UV-curing kinetics, with three kinds of initiators, and properties of the cured films were evaluated using real-time Fourier transform infrared (FTIR) spectroscopy, water and diiodomethane contact angle tests, surface energy calculations and scanning electron microscopy (SEM). The FTIR spectroscopy results showed that the coatings possessed excellent conversion rate (> 99% with liquid initiator PAG-201 in 150 s), and as the fluorine content increased, the monomers exhibited decreased mobility with the increasing viscosity and worse solubility with fluorinated monomers, resulting in a lower conversion rate. Moreover, the coatings possessed favorable hydrophobic and oleophobic properties and low surface energies owing to the fluoride chains floating to the membrane-air interface, which was also confirmed by discrete concave structures in SEM images. These new kinds of monomers can replace traditional fluorinated cationic monomers applied to the fingerprint resistant, fouling resistant, scratch resistant and anti-aging coatings, adhesives or printing ink materials.

**Keywords** Fluorine-containing monomers; Oxetane; UV-curing kinetics; Surface properties

**Citation:** Fang, S. Q.; Pang, Y. L.; Zou, Y. Q. Synthesis, UV-curing Behavior and Surface Properties of New Fluorine-containing Aromatic Oxetane Monomers. Chinese J. Polym. Sci. 2018, 36(4), 521–527.

## INTRODUCTION

With the rapid development of UV-curing technology, cationic UV-curing systems are attracting increased attention because of their outstanding advantages, namely, the lack of inhibition due to oxygen, low shrinkage, the good mechanical properties of the UV-cured materials and the good adhesion properties to various substrates[1, 2]. Compared to the epoxy and vinyl ether monomers of cationic UV-curing systems, oxetane monomers have high ring strain and high basicity of the heterocyclic oxygen, similar to the epoxy monomer, while possessing a lower viscosity, lower toxicity, higher curing rate and higher thermal stability[3, 4]. Thus, recently, much attention has been devoted to the synthesis and cationic photopolymerization of oxetane monomers and the properties of the corresponding polymers and hybrid-polymers[5–8]. However, at present, the oxetane monomers suitable for UV curing are not as numerous as the epoxy and vinyl ether monomers, and the choice is even narrower when dealing with fluorinated compounds.

With the rapid development of UV curing technology, it is necessary to improve the performance of UV-curing materials, such as corrosion resistance, fingerprint resistance, scratch resistance, dirt resistance and weather resistance[9]. In order to meet the above requirements, we introduced fluorinated alkyl chains into the oxetane monomers. Many papers have described that the introduction of perfluorinated chains can empower the hydrophobic and oleophobic abilities of polymers, consequently reducing the surface energy of polymer membranes[10–17]. Many research studies have been conducted to introduce fluoride oxetane monomers to other cationic or radical polymerization systems to obtain hybrid polymers that successfully change the surface properties of the base polymer[18–22]. Some papers have already presented results in which oxetane UV-cured systems were developed, either based on fluorinated oxetane monomers or containing small amounts of fluorinated monomers as additives (less than 1 wt%) to achieve surface modification[5, 10]. To date, most of the patents regarding fluoride oxetane monomers have been developed by Japanese companies. At the current stage, there are still demands to exploit new types of fluorinated oxetane monomers that can be used to develop high-end UV-curing systems.

Herein, four fluorine-containing aromatic oxetane monomers (FOX1–4) were synthesized *via* the reaction between 3-methyl-3-oxetanemethanol, the corresponding perfluorinated alcohol and hexafluorobenzene under the

* Corresponding author: E-mail zouyq@263.net
Received May 24, 2017; Accepted September 22, 2017; Published online December 20, 2017

catalysis of NaH[23]. The reaction occurred under mild conditions and produced a high yield and stable product. The structures and properties of the monomers were characterized using $^{1}$H-NMR, $^{19}$F-NMR, dynamic viscosity tests and differential scanning calorimetry (DSC). Subsequently, UV-curable coatings were prepared using FOX1–4; the UV-curing kinetics, with three kinds of initiators, and properties of the cured films were evaluated using real-time Fourier transform infrared (FTIR) spectroscopy, $H_2O$ and $CH_2I_2$ contact angle tests, surface energy calculations and scanning electron microscopy (SEM).

## EXPERIMENTAL

### Synthesis and Characterization of the Fluoride Oxetane Monomer

*Materials*

Hexafluorobenzene, sodium hydride (60% in mineral oil), 2,2,2-trifluoroethanol, 2,2,3,3,4,4,4-heptafluoro-1-butanol, 1H,1H-perfluorooctane-1-ol, and 3-methyl-3-oxetanemethanol were purchased from Alfa Aesar China Ltd. (Tianjin, China). These reagents were used without further purification. Sodium hydride was washed with petroleum immediately before use for removing the protective oil. Tetrahydrofuran (THF), petroleum ether and magnesium sulfate were provided by Beijing Chemical Reagent Company (Beijing, China). The THF was dried over sodium and distilled before use. The photo-acid generators (PAG) used in the experiments were as follows (Fig. 1). [4-(Phenylthio)phenyl]diphenylsulfonium-hexafluorophosphate (GR-SS-002) and mixed sulfonium-hexafluorophosphate (GR-SS-004) were purchased from Hubei Gurun Technology Co., Ltd. (Hubei, China). PAG-201 (a mixture of 4-thiophenyl phenyl diphenylsulfoniumhexa-fluoroantimonate, diphenyl (4-phenylthio)phenylsulfonium-hexafluoroantimonate and 2-oxo-4-methyl-1,3-dioxolane) was purchased from Shenzhen Rongda Photosensitive Science & Technology Co., Ltd. (Shenzhen, China).

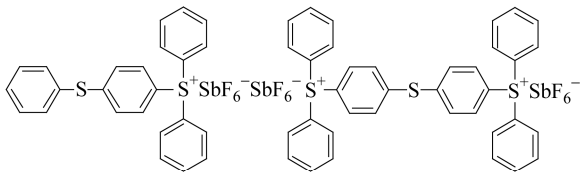

PAG-201

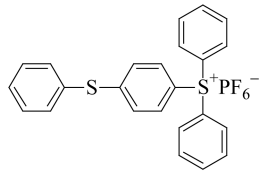

GR-SS-002

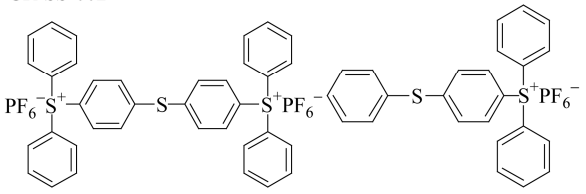

GR-SS-004

**Fig. 1** The chemical structures of the photoinitiators: PAG-201, GR-SS-002, and GR-SS-004

*The Synthesis of the Monomers*

The chemical structures of OX, FOX1, FOX2, FOX3, FOX4 are showed in Fig. 2. Take the synthesis route of FOX3 for example. Sodium hydride was washed with petroleum ether immediately before use for removing the protective oil. Under the protection of $N_2$, the activated sodium hydride (0.52 g, 0.013 mol) was dispersed in THF (50 mL) in an ice bath. 3-Methyl-3-oxetane methanol (1.224 g, 0.012 mol) was then added to the solution dropwise. The mixture was stirred in an ice bath for 1 h before the dropwise addition of hexafluorobenzene (1.86 g, 0.01 mol). The reaction mixture was then allowed to stir for 10 h at room temperature. Petroleum ether (3 × 50 mL) was used to extract the product. After washing with water (3 × 30 mL), the product was dried over anhydrous $MgSO_4$. Petroleum was removed using rotary evaporation, and a distillation under reduced pressure was then performed and product FOX1 was collected from 110–120 °C, 0.0033 MPa. 1H,1H-heptafluoro-1-butanol (2.323 g, 0.012 mol) and NaH (0.52 g, 0.013 mol) were diluted in 50 mL of THF and added to the FOX1 (2.68 g, 0.01 mol) in 30 mL of THF in ice bath and then the mixture was allowed to stir overnight. Petroleum ether (3 × 50 mL) was used to extract the product. After washing with water (3 × 30 mL) until the waste was neutral, the product was dried over anhydrous $MgSO_4$. The solvent was removed using rotary evaporation, and then, the residue was removed under reduced pressure (FOX1: 110–120 °C, 0.0033 MPa; 1H,1H-heptafluoro-1-butanol: 30–40 °C, 0.0033 MPa) to obtain the final pale yellow oily product, FOX3. High-performance liquid chromatography (HPLC) was operated on the LC-20A HPLC instrument (Shimadzu Corp., Tokyo, Japan). The chromatographic conditions were as follows: Diamonsil Plus 5 μm C18 column (5 μm, 150 mm × 4.6 mm) used as the stationary phase, ethanol-water (60/40, *V*/*V*) as mobile phase with a flow rate of 0.8 mL/min. Retention time of FOX3 was 23.5 min; purity was 95%.

The synthesis methods for FOX2 and FOX4 were the same as that of FOX3, as shown in Scheme 1.

NMR spectroscopy was performed using a Bruker AV (Bruker, Rheinstetten, Germany) spectrometer with a probe frequency of 500 MHz for $^{1}$H and $^{19}$F observation.

FOX1, light-yellow liquid, yield: 95%, 3-methyl-3-((perfluorophenoxy)methyl)oxetane; $^{1}$H-NMR ($CDCl_3$, TMS, $\delta$, ppm): 4.62 (d, 2H), 4.46 (d, 2H), 4.2 (s, 2H), 1.45 (s, 3H); $^{19}$F-NMR ($CDCl_3$, TMS, $\delta$, ppm): −156.1 (d, 2F), 160.6 (m, 1F), −162.5 (d, 2F).

FOX2, pale-yellow liquid, yield: 85%, 3-methyl-3-((2,3,5,6-tetrafluoro-4-(2,2,2-trifluoroethoxy)phenoxy)methyl)oxetane; $^{1}$H-NMR ($CDCl_3$, TMS, $\delta$, ppm): 4.63 (d, 2H), 4.58 (m, 2H), 4.48 (d, 2H), 4.24 (s, 2H), 1.45 (s, 3H); $^{19}$F-NMR ($CDCl_3$, TMS, $\delta$, ppm): −75.2 (s, 3F), 156.4 (d, 2F), 162.5 (d, 2F).

FOX3, yellow liquid, yield: 86%, 3-methyl-3-((2,3,5,6-tetrafluoro-4-(2,2,3,3,4,4,4-heptafluorobutoxy)phenoxy)methyl)oxetane; $^{1}$H-NMR ($CDCl_3$, TMS, $\delta$, ppm): 4.63 (d, 2H), 4.58 (m, 2H), 4.48 (d, 2H), 4.24 (s, 2H), 1.45 (s, 3H); $^{19}$F-NMR ($CDCl_3$, TMS, $\delta$, ppm): −81.04 (s, 3F), 123.9 (s, 2F), 128.9 (s, 2F), −157.2 (d, 2F), 163.0 (d, 2F).

https://doi.org/10.1007/s10118-018-2048-4

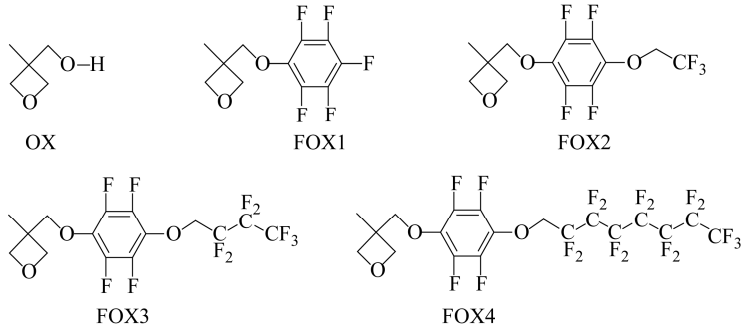


**Fig. 2** The chemical structures of monomers OX, FOX1, FOX2, FOX3, and FOX4

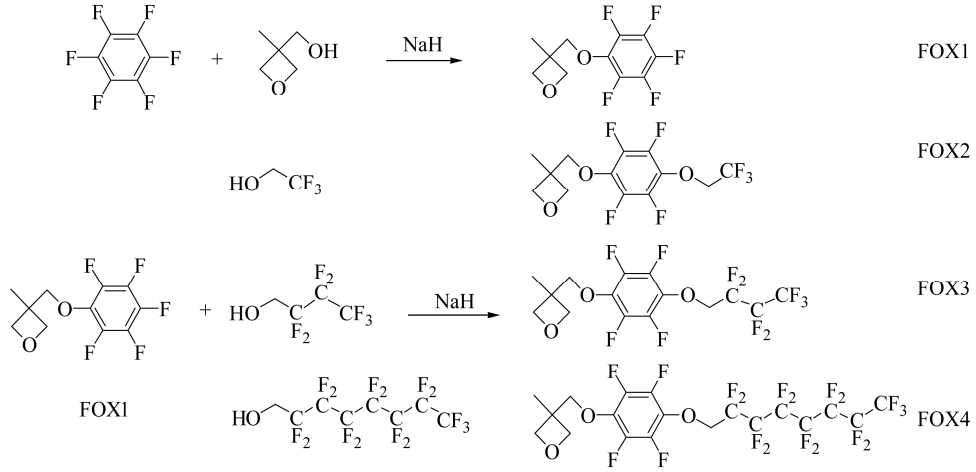


**Scheme 1** The synthesis routes of FOX1, FOX2, FOX3, FOX4

FOX4, brown liquid (20 °C), yield: 84%, 3-methyl-3-((2,3,5,6-tetrafluoro-4-((2,2,3,3,4,4,5,5,6,6,7,7,8,8,8-pentadecafluorooctyl)oxy)phenoxy)methyl)oxetane; $^1$H-NMR ($CDCl_3$, TMS, $\delta$, ppm): 4.61 (d, 2H), 4.58 (m, 2H), 4.46 (d, 2H), 4.21 (s, 2H), 1.44 (s, 3H); $^{19}$F-NMR ($CDCl_3$, TMS, $\delta$, ppm): –80.97 (s, 3F), 121.2 (s, 2F), 122.5 (s, 2F), 123.8 (s, 2F), 125.2 (s, 2F), 127.5 (s, 2F), 157.2 (d, 2F), 163.2 (d, 2F).

The dynamic viscosity of the monomer was measured using a capillary viscometer (NDJ-01, Huaqiao Glass Instrument, Shenyang) in a thermostatic water bath (25 °C). The thermal stability of these monomers was measured by conducting a thermogravimetric analysis (Mettler-Toledo TGA/DSC 1/1100 instrument). The weight of the monomer samples was 5 mg, and the specimens were placed in an aluminum pan and heated at a heating rate of 10 K/min from room temperature to 600 °C in $N_2$.

**Characterization of the UV-curing Kinetics**

RT-FTIR was used to investigate the kinetics of the UV-cured polymerization. The light source was a 200 W high-pressure mercury lamp with a wavelength range of 300–440 nm. The UV light intensity on the sample was 40 mW/cm$^2$. The photopolymerizable mixtures were prepared from (0.5 ± 0.01) g of monomer, 5.0 wt% initiator, and 1 mL of acetone. The solvent contained in the sample was evaporated for over 5 min before UV curing.

**Preparation and Characterization of the Cured Film**

The films were obtained by coating the photopolymerizable mixtures mentioned above on glass slides. The mixtures were spread on a glass slide with a calibrated wire-wound applicator to obtain 100 μm thick film. The solvent was evaporated in air. The curing reaction was performed using UV irradiation with a fusion lamp that produced a radiation intensity of 280 mW/cm$^2$ on the surface of the sample for 3 min. Static contact angle measurements were carried out at room temperature using a contact angle analyzer (OCA15-EC, Data Physics Instruments, Germany). The sessile drop technique (each droplet volume was *ca*. 2 μL) was used together with a video camera and image analyzer. The liquids used for measurements were twice-distilled water and diiodomethane. The temperature and relative humidity were (23 ± 1.5) °C and (55 ± 5)%, respectively. At least five measurements were obtained for each film, and the deviation from the average was less than 3°.

The surface energy was calculated according to Owens-Wendt and Young's equations. In the Owens-Wendt equation, the surface energy ($\gamma$) is the sum of the dispersion forces ($\gamma^d$) and the polarity forces ($\gamma^p$). The dispersion ($\gamma^d$) and polarity forces ($\gamma^p$) are calculated by the following equation (Eq. 1).

$$\gamma^d = \frac{1}{\gamma_{dim}^d} \times \left[ \frac{\gamma_{dim} \times (\cos\theta_{dim} + 1)}{2} \right]^2$$

$$\gamma^p = \left[ \frac{\gamma_w \times (\cos\theta_w + 1)}{2} - \frac{\gamma_{dim} (\cos\theta_{dim} + 1)}{2} \right] \times \left[ \frac{\gamma_w^d}{\gamma_{dim}^d} \right]^{0.5} \quad (1)$$

$\gamma_w$ = 72.8 mJ/m$^2$, $\gamma_w^d$ = 21.8 mJ/m$^2$, $\gamma_{dim}$ = 50.8 mJ/m$^2$, $\gamma_{dim}^d$ = 50.8 mJ/m$^2$.

https://doi.org/10.1007/s10118-018-2048-4

The surface of the cured film was observed using scanning electron microscopy (SEM, Hitachi S-4800 FESEM) with the accelerating voltage of 10 kV. For SEM inspection, the samples were fixed to aluminum stubs with conductive tape.

## RESULTS AND DISCUSSION

### Synthesis of the Monomers

The fluorinated oxetane monomers were synthesized by a nucleophilic substitution reaction between the fluorinated alcohols and oxetane in the presence of NaH. Two types of fluoride alcohol were investigated, and the results showed that HO—$CH_2$—$C_nF_{2n+1}$ was produced with a higher yield than HO — $CH_2$ — $CH_2$ — $C_nF_{2n+1}$. Owing to the higher reactivity of the O atoms of the hydroxyl groups, which were closer to the —$CF_2$— groups, the nucleophilic substitution reactions were more likely to occur.

### Viscosity and Thermal Stability of the Monomers

The viscosities of OX and the fluorinated monomer were measured using a viscometer. As can be seen in the Table 1, the viscosity of the raw material was high and reached 20.67 $mm^2/s$ compared to FOX1 with a viscosity of 4.58 $mm^2/s$. The main reason is that the replacement of hydroxyl by alkyl could lead to the disappearance of intermolecular hydrogen bond and thus reduce viscosity. In addition, as the molecular weight increased from the FOX1 to FOX4 monomer, the dispersion force increased, resulting in stronger intermolecular forces and higher viscosity. Moreover, Table 1 also shows the temperature of 10% weight loss and 50% weight loss of monomers. It is obvious that the thermal stability of the monomers was enhanced by introducing aromatic rings and fluorinated alkyl chains. Hence, imparting the physical properties of low viscosity and thermal stability satisfied the material requirements for developing UV-imaging materials.

**Table 1** The fluorine content (FC), viscosity and temperature at 10% weight loss and 50% weight loss

| Monomer | FC (wt%) | Viscosity at 25 °C ($mm^2/s$) | Temperature at 10% weight loss (°C) | Temperature at 50% weight loss (°C) |
|---|---|---|---|---|
| OX | 0 | 20.67 | 118 | 155 |
| FOX1 | 35.4 | 4.58 | 131 | 179 |
| FOX2 | 40.1 | 5.22 | 169 | 212 |
| FOX3 | 46.6 | 6.73 | 180 | 221 |
| FOX4 | 55.7 | 15.62 | 202 | 253 |

### Kinetics of UV-curing

The UV-curing kinetics of the fluorinated oxetane monomers were measured using RT-FTIR, and the UV-light intensity was 40 $mW/cm^2$. In the cationic UV-curing system, the photoinitiator produced a strong proton acid under ultraviolet excitation, prompting the cyclobutane rings to open their loops and produce active centers[24]. Then, the activity centers caused other monomers to undergo ring-opening polymerization, as shown in Scheme 2. As a result, the FOX monomer was photopolymerized in the presence of the activity centers. Owing to the high ring strain energy of 107 kJ/mol and high basicity with a p$K_a$ of 3.7, the rate of polymerization for the oxetane rings was higher than that of the cycloaliphatic epoxy monomer.

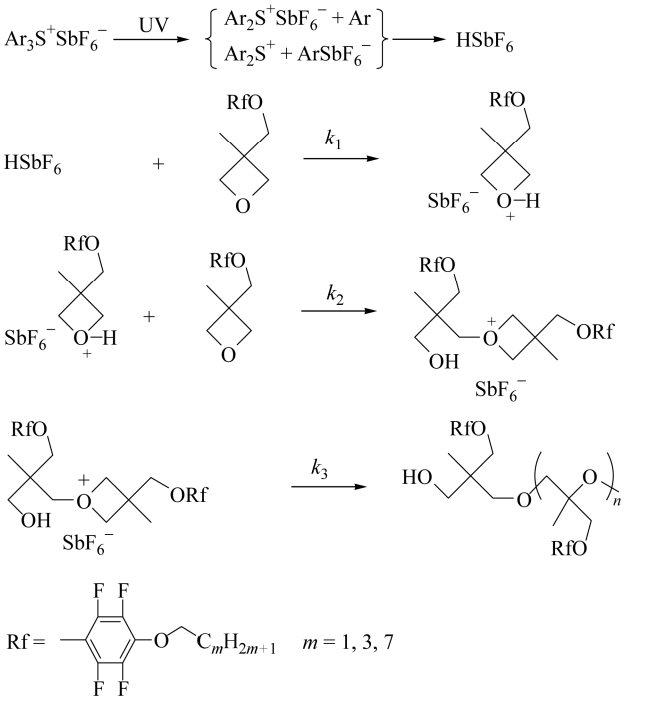


**Scheme 2** The photocuring process of fluorine-containing aromatic oxetane monomers

Conversion data were obtained by monitoring the decay of the typical oxetane IR band at approximately 830 $cm^{-1}$. Upon irradiation, the decrease in the absorption peak area accurately reflected the extent of polymerization. The decrease in the absorption peak area was directly proportional to the number of oxetane rings that had been polymerized. The degree of conversion (DC) of the functional groups could be calculated by measuring the peak area at each time point of the reaction and determined using the following equation:

$$\mathrm{DC}\ (\%) = \frac{(A_0 - A_t)}{A_0} \times 100 \qquad (2)$$

where DC is the conversion at time $t$, and $A_0$ and $A_t$ are the peak areas of the functional groups before irradiation and at time $t$, respectively. In order to find a photoinitiator suitable for the fluorinated oxetane monomers, three kinds of UV-light initiators, named PAG-201, GR-SS-002, and GR-SS-004, were used in the experiments. Figures 3(a)–3(d) show the conversion rate versus time curves for FOX1, FOX2, FOX3, and FOX4, initiated using PAG-201, GS-SS-002, and GS-SS-004.

As can be seen, the conversion rate and conversion speed of the three kinds of photoinitiators were ranked as follows: PAG-201 > GR-SS-004 > GR-SS-002. In Fig. 4, all monomers initiated using PAG-201 possessed a high conversion rate, reaching over 99% in less than 150 s. However, the monomer initiated by GR-SS-002 and GR-SS-004 had lower conversion rates and speeds. It was mainly because fluorine-containing substances had bad solubility with solid salt initiators. Undissolved solid particles

https://doi.org/10.1007/s10118-018-2048-4

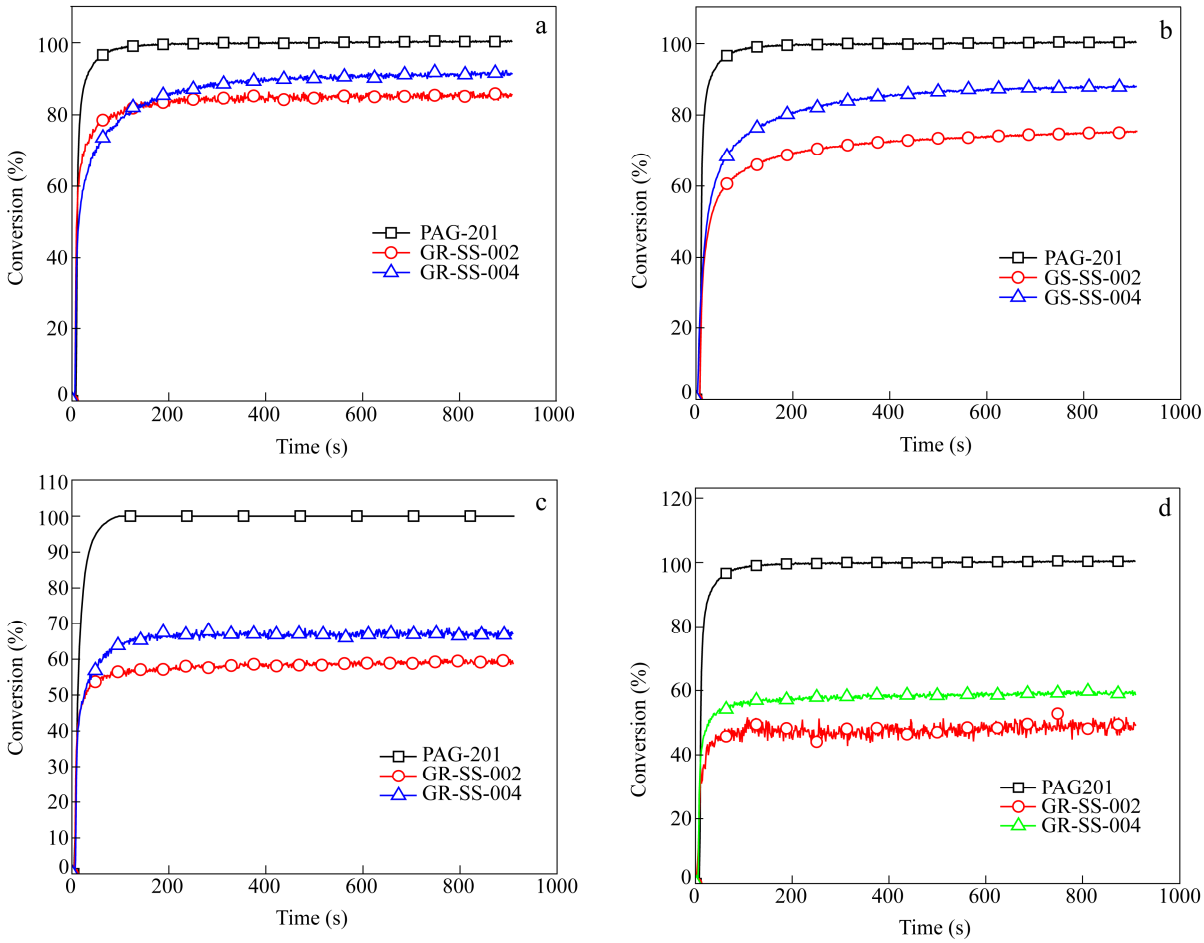


**Fig. 3** Conversion curves versus time for the FOX1 (a), FOX2 (b), FOX3 (c), and FOX4 (d) monomers initiated by 5.0 wt% PAG-201, GS-SS-002, and GS-SS-004 ($I$ = 40 mW/cm$^2$)

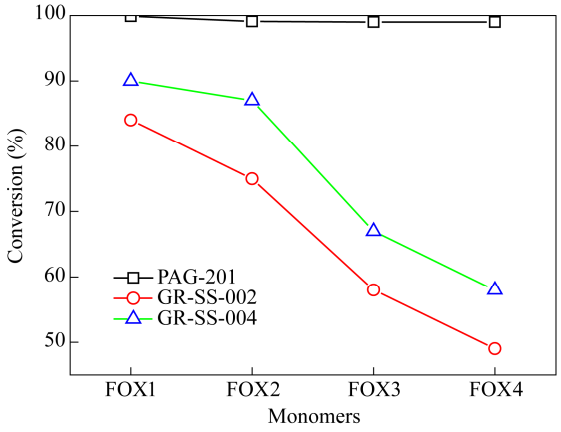


**Fig. 4** The conversion differences between monomers FOX1 to FOX4 using the same initiators (5.0 wt%, $I$ = 40 mW/cm$^2$)

could be observed in the mixture after solvent evaporation, which means that part of light initiators did not work at all. However, PAG201 is a mixture of 4-thiophenyl phenyldiphenylsulfoniumhexafluoroantimonate, diphenyl(4-phenylthio)phenylsulfoniumhexafluoroantimonate and 2-oxo-4-methyl-1,3-dioxolanen, which augments the solubility between the salt initiator and monomer as an efficient solvent with respect to the solid initiators (GR-SS-002 and GR-SS-004). In addition, in Fig. 4, as the perfluorinated chains grew longer (increasing FC) from FOX1 to FOX4, the monomers initiated by GR-SS-002 and GR-SS-004 exhibited lower final conversion rates because of their worsening solubility and mobility with the increasing viscosity. So in summary, PAG-201 among the three kind of initiators was the most suitable option for this kind of fluorinated oxetane monomers. And the good solubility between monomers and initiators, and low viscosity were beneficial for UV-curing. Thus, in the following experiment, PAG-201 was used in all recipes.

## Surface Properties

To investigate the effects of the perfluorinated alkyl groups on the surface properties of the polymerized films, contact angle measurements were performed with deionized water and $CH_2I_2$ as wetting agents. The films were obtained by coating the photopolymerizable mixtures ((0.5 ± 0.01) g fluorinated monomer, 5.0 wt% initiator, 1 mL acetone) mentioned above on glass slides. The surface free energy values of the films were calculated from the average contact angles.

As shown in Table 2, with the increasing fluorine content, the surfaces of the polymers became hydrophobic and oleophobic. As expected, the surface tension of the films decreased significantly compared to poly-OX. The contact angle of poly-FOX3 reached 112.5° for water and 73° for $CH_2I_2$. Oleophobic properties were harder to achieve than

https://doi.org/10.1007/s10118-018-2048-4

**Table 2** Surface energy parameters of the UV-cured films

| Sample | Fluorine content (wt%) | Contact angle (°) | | Surface energy [d] (mJ/m$^2$) | | |
|---|---|---|---|---|---|---|
| | | $\theta_w$ [a] | $\theta_{dim}$ [b] | $\gamma^{d}$ [c] | $\gamma^{p}$ [d] | $\gamma$ [e] |
| Poly-OX | 0 | 62 ± 2.0 | 59.8 ± 1.7 | 28.8 | 10.0 | 38.8 |
| Poly-FOX1 | 35.4 | 95.6 ± 2.3 | 65.9 ± 1.9 | 25.5 | –2.0 | 23.5 |
| Poly-FOX2 | 40.1 | 98.5 ± 1.5 | 66.1 ± 1.5 | 25.2 | –3.1 | 22.1 |
| Poly-FOX3 | 46.6 | 112.5 ± 2.4 | 73.7 ± 2.1 | 21.0 | –6.6 | 14.4 |
| Poly-FOX4 | 55.7 | 122.5 ± 2.7 | 91.4 ± 3.2 | 12.2 | –5.2 | 7.0 |
| Glass | – | 21.8 ± 1.4 | 47.4 ± 2.6 | 36.6 | 18.3 | 54.9 |

[a] The contact angle of $H_2O$; [b] The contact angle of $CH_2I_2$; [c] $\gamma^{d}$ = dispersion force; [d] $\gamma^{p}$ = polarity force; [e] $\gamma$= surface energy

hydrophobic properties because of the higher surface energy of water.

After the cured film of the polymer was removed, the water contact angle of the glass-polymer side was also measured for comparison with the air-polymer side, as shown in Fig. 5. The contact angle of the air side of the polymer with the fluorinated alkyl chains was larger than that of the glass side, especially for poly-FOX2 and poly-FOX3, indicating that the fluoride segments gathered at the polymer-air layer (Fig. 6). The SEM images also confirmed the result (Fig. 7). The cured surfaces of the poly-FOX1, poly-FOX2, and poly-FOX3 were uniform and smooth, while poly-FOX4 had a rough and uneven surface at the macro-scale. In the SEM images, the surface of poly-FOX1, which contained only hexafluorobenzene structure and no fluorinated alkyl chains, was smooth and even. However, in SEM images of poly-FOX2 and poly-FOX3, discrete concave structures were observed. This phenomenon was typical microphase separation caused by fluorinated alkyl chains migrating to the film surface, which had been observed in many fluorine-containing UV-curing system[4, 18]. Due to the relatively high fluorine content of every sample and high density of monomer, the discrete concave was compact and deep. Because of their relatively low surface energy, the fluorinated monomers had a tendency to move toward the polymer-air interface. Therefore, there are two main reasons for the reduction of surface energy: (1) The fluorine atoms gathered on the polymer-air interface; (2) These discrete concave or uneven surface increased the contact angle of water and $CH_2I_2$ thus decreased surface energy[10].

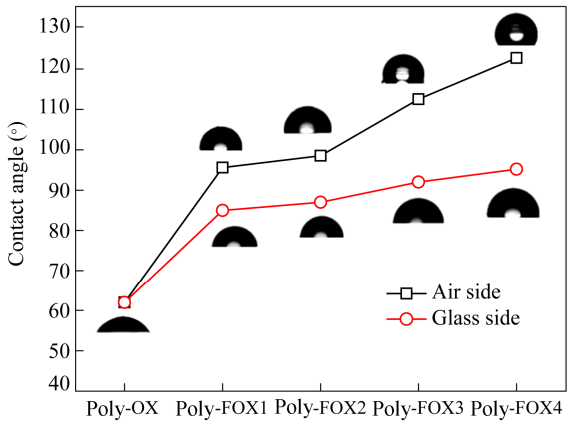


**Fig. 5** The water contact angles on the surfaces of the polymers from different monomers on the air side and glass side

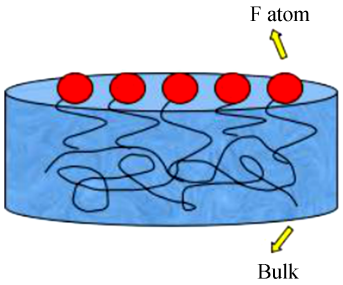


**Fig. 6** The fluoride segments gathered at the polymer-air layer

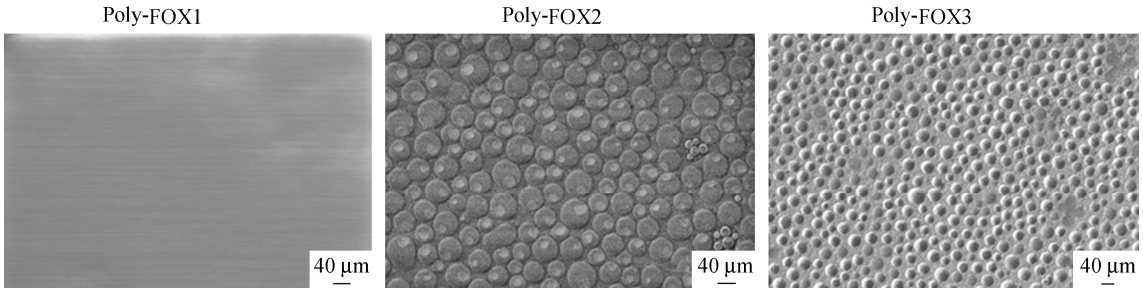


**Fig. 7** SEM images of the poly-FOX1, poly-FOX2 and poly-FOX3 surfaces

## CONCLUSIONS

Four fluorine-containing aromatic oxetane monomers (FOX1–4) were synthesized *via* nucleophilic substitution reactions between 3-methyl-3-oxetanemethanol, the corresponding perfluorinated alcohol and hexafluorobenzene under the catalysis of NaH. The monomers exhibited excellent physical properties, low viscosity and high thermal stability, which satisfied the material requirements for UV-imaging materials. UV-curable coatings were prepared from FOX1–4, and FTIR measurements indicated that these coatings possessed excellent conversion (> 99% with liquid

https://doi.org/10.1007/s10118-018-2048-4

initiator PAG-201). As the fluorine content increased, the monomers exhibited decreased mobility with the increasing viscosity, resulting in lower conversion rates. The curing efficiency of the fluorinated monomers was related to the viscosity of the monomers and their solubility with the initiators. Low viscosity and good solubility were beneficial for UV-curing.

Concerning the surface properties of the cured films, the fluorinated polymers exhibited very high hydrophobic and oleophobic characteristics and low surface energies, as expected. The SEM images evidenced selective enrichment of the fluorinated segments at the air surface, as previously shown for other photocured systems.

## ACKNOWLEDGMENTS

This work was financially supported by the National Natural Science Foundation of China (No. 21574014).

## REFERENCES

1 Sangermano, M.; Bongiovanni, R.; Malucelli, G.; Priola, A.; Thomas, R. R.; Medsker, R. E.; Kim, Y.; Kausch, C. M. Synthesis and cationic photopolymerization of a new fluorinated oxetane monomer. Polymer 2004, 45(7), 2133–2139.
2 Yang, J.; Huang, W. Y. Synthesis and characterization of a novel fluorine-containing hydrophobically associating polymer. Chinese J. Polym. Sci. 1999, 17(3), 281–288.
3 Wan, S. C.; Huang, B. W.; Du, Z. P. Study on the synthesis of 3,3'-[1,4-butanediylbis(oxymethylene)]bis[(3-ethyl)oxetane] for the novel cationic curing monomer. Imag. Sci. Photochem. 2016, 181–189.
4 Kurt, P.; Wynne, K. J. Co-polyoxetanes with alkylammonium and fluorous or PEG-like side chains: soft blocks for surface modifying polyurethanes. Macromolecules 2007, 40(26), 9537–9543.
5 Škola, O.; Jašúrek, B.; Veselý, D.; Němec, P. Mechanical properties of polymer layers fabricated *via* hybrid free radical-cationic polymerization of acrylate, epoxide, and oxetane binders. Prog. Org. Coat. 2016, 101, 279–287.
6 Nakano, Y.; Tsutsumi, H. Ion conduction and electrochemical performance of poly(oxetane)-based electrolytes with tri(cyanoethoxymethyl) moiety as a side chain. ECS Transactions 2014, 62(1), 255–263.
7 Zhan, F.; Cheng, X.; Shi, W. F. Synthesis and properties of oxetane-based polysiloxanes used for cationic UV curing coatings. Polym. Adv. Technol. 2012, 23(3), 645–651.
8 Bongiovanni, R.; Malucelli, G.; Sangermano, M.; Priola, A. Fluorinated networks through photopolymerisation processes: synthesis, characterisation and properties. J. Fluorine Chem. 2004, 125(2), 345–351.
9 Mou, H.; Chen, L.; Wang, C.; Wang Y. L.; Wang, X. L. Paint Coat. Ind. 2015, 2, 1–6.
10 Tan, J. Q.; Liu, W. Q.; Wang, Z. F. Preparation and performance of waterborne UV-curable polyurethane containing long fluorinated side chains. J. Appl. Polym. Sci. 2017, DOI: 10.1002/app.44506
11 Liu, B.; Bao, Y.; Ling, H. F.; Zhu, W. S.; Gong, R. J.; Lin, J. Y.; Xie, L. H.; Yi, M. D.; Huang, W. Fluorinated p-n type copolyfluorene as polymer electret for stable nonvolatile organic transistor memory device. Chinese J. Polym. Sci. 2016, 34(10), 1183–1195.
12 Li, W.; Feng, P.; Zou, Y. Q.; Hai, B. Synthesis and cationic photopolymerization of fluorine-containing vinyl ether monomers for the hydrophobic films. J. Appl. Polym. Sci. 2014, 131(21), 41019.
13 Li, W.; Zou, Y. Q. Synthesis, UV-curing behavior and surface properties of fluorine-containing vinyl ether polymers. Chinese J. Polym. Sci. 2014, 32(8), 1032–1039.
14 Canak, T. C.; Hamuryudan, E.; Serhatli, I. E. Synthesis and characterization of perfluorinatedacrylatemethyl methacrylate copolymers. J. Appl. Polym. Sci. 2013, 128(3), 1450–1461.
15 Lin, Y.; Liao, K.; Huang, C.; Chou, N.; Wang, S.; Chu, S.; Hsieh, K. Superhydrophobic films of UV-curable fluorinated epoxy acrylate resins. Polym. Int. 2010, 59(9), 1205–1211.
16 Wang, J.; Huang, J. Q.; Huang Y. G.; Qing, F. L. Synthesis and characterization of novel oxetane monomers containing short perfluorocarbon side chains. Chinese J. Org. Chem. 2009, 1969–1974.
17 Xie, K.; Hou, A.; Shi, Y. Synthesis of fluorine-containing acrylate copolymer and application as resinson dyed polyester microfiber fabric. J. Appl. Polym. Sci. 2008, 108(3), 1778–1782.
18 Kurt, P.; Chakravorty, A.; Zeng, X. M.; Wynne, K. J. Strongly amphiphilic wetting behavior for polyurethanes with polyoxetane soft blocks having $-CF_2H$ terminated side chains. Polymer 2014, 55(9), 2170–2178.
19 Deng, C.; Xie, W. F.; Huang, B. W. Study on the properties of oxetane/acrylate UV-cured hybrid system. Imag. Sci. Photochem. 2014, 289–299.
20 Yang, S.; Jin, J.; Kwak, S.; Bae, B. Photocurable transparent cycloaliphatic epoxy hybrid materials crosslinked by oxetane. J. Appl. Polym. Sci. 2012, 126(S2), E380–E386.
21 Zhan, F.; Zhang, Y.; Shi, W. F. Synthesis of perfluorinated oxetane and surface properties of its cationic UV cured coating as a reactive additive. Chem. Res. Chinese U. 2012, 28(3), 550–558.
22 Ertekin, A.; Kim, Y.; Kausch, C. M.; Thomas, R. R. Adsorption properties of oligo(fluorooxetane)-*b*-poly(ethylene oxide)-*b*-oligo(fluorooxetane) triblock copolymers at the air-water interface: comparison of hydroxyl and acetate end groups. J. Colloid Interf. Sci. 2009, 336(1), 40–45.
23 Song, B. J.; Park, J. K.; Kim, H. K. Novel photocurable multifunctional acrylate monomers containing perfluorinated aromatic units and their copolymers for photonic applications. J. Polym. Sci., Part A: Polym. Chem. 2004, 42(24), 6375–6383.
24 Liu, H. T.; Mo, J. H.; Liu, H. C. HuaZhong U. Sci. Technol., Nat. Sci. Ed. 2008, 36, 129–132.